Offset Aperture-Coupled Double-Cylinder Dielectric Resonator Antenna with Extended Wideband

C.-E. Zebiri, M. Lashab, D. Sayad, I.T.E. Elfergani, K.H. Sayidmarie, F. Benabdelaziz, R.A. Abd-Alhameed, J. Rodriguez, J.M. Noras

***Abstract*—A compact dielectric resonator antenna for ultra-wideband vehicular communication applications is proposed. Two cylindrical dielectric resonators are asymmetrically located with respect to the center of an offset rectangular coupling aperture, through which they are fed. Optimizing the design parameters results in an impedance bandwidth of 21%, covering the range from 5.9 to 7.32 GHz in the lower-band and a 53% relative bandwidth from 8.72 to 15 GHz in the upper-band. The maximum achieved gain is 12 dBi. Design details of the proposed antenna and the results of both simulations and experiment are presented and discussed.**

***Index Terms*—Dielectric Resonator Antenna (DRA), aperture coupling, asymmetric shape**

I. Introduction

Antenna applications for vehicular communications have attracted much interest in the last decade [1-3]. Coverage of the required frequency range of 6 to 10 GHz has made use of various structures derived from the UWB field. A microstrip patch antenna with defected ground structure was used for cross polarization suppression in [4], in [5] to improve polarization purity, and in [6] to reduce mutual coupling between two CDRAs. A new technique to excite a higher order radiating mode for CDR was demonstrated in [7], and recently a dual band CDRA employing two hybrid modes excited by a new composite aperture was illustrated in [8]. Defected ground structures have been used for the control of active microstrip antennas and bandwidth enhancement techniques in patch antennas [9].

Moreover, DRAs with various geometries such as conical [10], cylindrical [11] (for first use as a cylindrical radiating element see [12]), asymmetrical T-shaped [13], tetrahedral [14], ring-shaped [6], elliptical [15], and hybrid hemispherical-conical-shaped [16]: these are all structures proposed for bandwidth enhancement. Recently, the operating DRA bandwidth was extended further for ultra-wideband applications [15-16]. In [17] a single cylindrical DR was excited by two crossed slots in which a wider band was attained. In [11], a novel wideband slot-fed asymmetric DR antenna was proposed, with two adjacent cylindrical DRs placed asymmetrically with respect to the feeding rectangular aperture. By optimizing the design parameters, an impedance bandwidth of about 46%, covering the frequency range from 9.1 to 14.6 GHz, and a simulated gain of 8 dBi has recently been achieved [18]. This technique can be applied to a large variety of transmission lines, including the conventional rectangular waveguide [19] and various planar waveguides such as the line strip [20, 21], coplanar waveguide [22], and substrate integrated waveguide [23]. One distinct advantage of aperture-fed DRAs is the easy realization of the desired polarization, which can be directly implemented either by selecting suitable slot shapes [24-26] or by adjusting the position and separation of slots.

The rectangular slot has been used extensively for the excitation of DR antennas. In addition to this form, there are other regular forms such as alphabetic slots [27], and more commonly circular [28-31], elliptical [31] and annular slots. In [28] an approach to enhance the bandwidth of a rectangular DR antenna using a large circular slot was exploited. It was found by using a (35 mm radius) circular slot rather than a (44 mm × 2 mm) rectangular slot, that a bandwidth of 36.44% (0.92 to 1.33 GHz) – in comparison to 6.39% (1.06 to 1.13 GHz) - was accomplished, with a similar radiation pattern. The circular slots have also been used as a coupler [29], and also as a radiator [28, 30, 31].

The asymmetric location of the DR pair constitutes an additional optimization parameter for the designer. The features of an antenna can be improved as in [11] where an impedance bandwidth of about 29%, covering the frequency range from 9.62 to 12.9 GHz, and a gain of 8 dBi were obtained. In the present work, for the same structure studied in [11] and with a large slot concept, this ratio increases by up to 100%. Bands of interest here are radio frequencies from 5.9 to19.57 GHz, and also earth-to-satellite bands (from 5.9 to 6.4 GHz, 12.25 to 13.25 GHz, and 14 to 14.5 GHz) and connections for satellite-earth at 10.7 to 11.7 GHz. Also relevant are the X-band of 8 to 12 GHz, 10.5 GHz for police radar, commercial use from 10.7 to 13.2 GHz, and finally the Ku-band at 12 to 18 GHz.

II. Proposed Antenna Geometry Summarized Results

In an attempt to increase the bandwidth of the DR antenna, an asymmetric location of two DRs on two adjacent slots were used. The UWB antenna was designed and simulated using HFSS V.14. The final configuration of the antenna, with an FR4 substrate of thickness 0.8 mm, is shown in Fig. 1. The prototype was fabricated on an FR4 substrate with a relative

This work is partially supported by the European Union's Horizon 2020 research and innovation programme under grant agreement H2020-MSCA-ITN-2016 SECRET-722424 and TSB-KTP project grant No. 008734 UK.

C.-E. Zebiri, M. Lashab, and D. Sayad are with the Department of Electronic, University of Ferhat Abbas, Sétif, Algeria.

F. Benabdelaziz, is with the Department of Electronic, University of Mentouri, Constantine, Algeria.

I.T.E. Elfergani,and J. Rodriguez are with Instituto de Telecomunicações – Aveiro, Campus Universitário de Santiago, Aveiro, Portugal.

K. H. Sayidmarie, is with the college of Electronic Engineering, Ninevah University, Mosul, Iraq.

R.A. Abd-Alhameed, J.M. Noras are with School of Electrical Engineering and Computer Science, University of Bradford, BD7 1DP, UK (e-mail: r.a.a.abd@bradford.ac.uk).

permittivity of ε_{rs} = 4.5, a loss tangent of 0.017 and a thickness t = 0.8 mm. The microstrip feed line, placed symmetrically with respect to the coupling aperture, has dimensions calculated using empirical formulas given in [11, 15] resulting in length l_f = 20.5 mm and width w_f = 1.5 mm. Two rectangular apertures (slots) of length l_s and width w_s were etched in the ground plane, shifted from the center of the feed line by a distance d. Practical experience has shown that the stub length should be close to $\lambda_g/4$ [32]. The values of the parameters in the final antenna configuration of Fig. 1 are (all in mm): w_g = 25, l_g = 30, w_f = 1.5, l_f = 21, w_s = 3.5, l_s = 6.6, d_s = 3.1, d = 0.2, l_{stub1} = 7.9 and l_{stub2} = 4.8. An alumina material, with ε_{rd} = 9.4, diameter D = 6 mm and height h = 9 mm was used for the DR structure.

In this section, different shapes of the aperture are studied in order to observe their effect on the reflection coefficient and bandwidth. Fig. 2 presents five configurations of the aperture starting from the very basic rectangular shape shown in Fig. 2a. Building on the previous work [11], the originality of the current work lies in the creation of two adjacent large slots combined with two cylindrical DRAs to excite further modes.

The two slots form a zigzag shape where "shifting the zigzag" gives design scope: one can also expand the slot, as shown in Fig. 2e. This figure shows the evolution of the desired slot shape. This original antenna provides an enhancement of S_{11}, as illustrated in Fig. 3. Fig. 2 and Fig. 3 show that slot length has the most effect on the reflection coefficient and the resonant frequency, but to a lesser extent, it also affects the impedance bandwidth of the antenna [11].

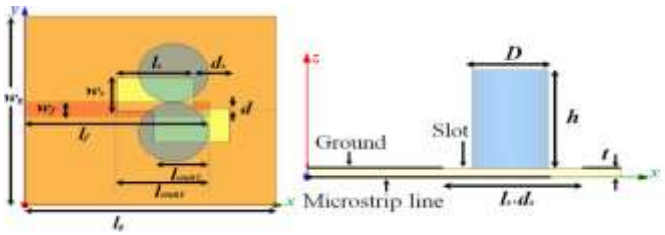

(a) (b)

Fig. 1: Aperture-coupled asymmetric DRA; (a) top view and (b) side view with design parameters shown.

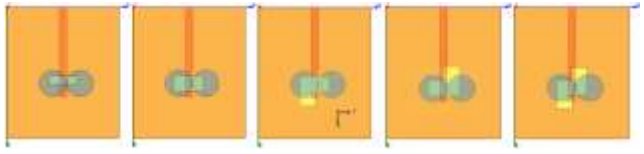

(a) (b) (c) (d) (e)

Fig. 2: Top view of an aperture-coupled asymmetric DRA: (a) antenna proposed in [11], (b)-(d) steps of evolution, and (e) final design of the present antenna.

The resonant frequency of a single segment CDRA exited in $HEM_{11\delta}$ mode can be derived from [11, 26, 33]:

$$f_r = \frac{c}{2a\pi\sqrt{\varepsilon_r}}\left(1.71+\frac{a}{h}+0.1578\left(\frac{a}{h}\right)^2\right) \quad (1)$$

where a = D/2, c is the velocity of light, with the other values given above. For these dimensions and with the DRA properties, the calculated resonance frequency is 10.63 GHz [4, 8], determined by the permittivity and dimensions of the DRs. Since the DRs are asymmetrically located with respect to the asymmetrical slots, we have two stub lengths l_{stub1} and l_{stub2}, where the actual DRA modes depend on the DR dimensions and the permittivity, as well on as the feeding mechanism. Thus several resonant frequencies are excited leading to effectively wideband operation.

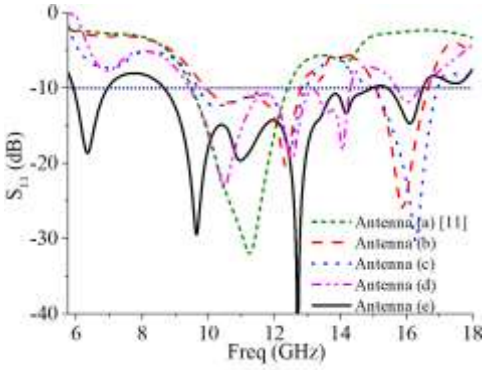

Fig. 3: Simulated reflection coefficients of the five antennas using the five slot shapes shown in Fig.2.

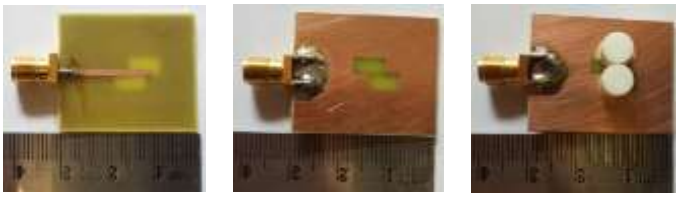

(a) (b) (c)

Fig. 4: Photograph of the fabricated antenna (a) front view, (b) rear view and (c) with the DRs.

Based on the detailed parametric study performed in [11], the optimum dimensions for the antenna given above are used in the fabrication of the antenna shown in Fig. 4.

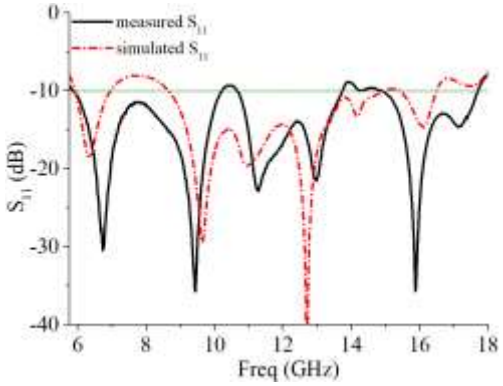

Fig. 5: Simulated and measured reflection coefficients of the DRA.

The antenna performance was measured with an HP8510C vector network analyzer, and the measured and simulated reflection coefficients of the antenna are shown in Fig. 5. The

comparison shows that there is better agreement for frequencies higher than 9 GHz. The differences between the measured and simulated results, seen in a shift towards higher frequencies and a general increase in S_{11}, can be attributed to the combined effects of the use of glue fixing the DRA and fabrication inaccuracy. The antenna demonstrates an impedance matching (S_{11}< -10 dB band) extending from 5.9 to 7.32 GHz (21.5% relative bandwidth), and from 8.72 to 15 GHz, (53% relative bandwidth).

Fig. 6 depicts the simulated and measured impedances for the antenna. The real parts are around 50 Ω, while the imaginary parts fluctuate around zero. The slight differences between the simulated and measured impedances are mainly due to fabrication errors.

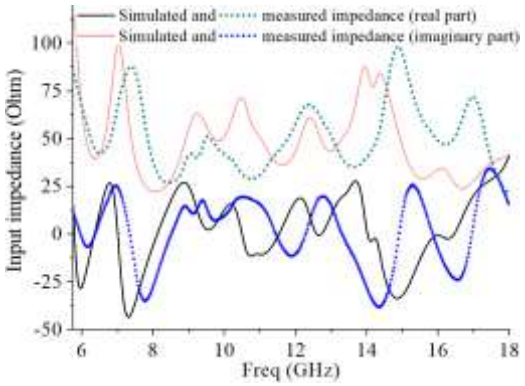

Fig. 6 Simulated and measured impedance of the antenna.

Fig. 5 and 6 indicate that several modes are excited and this is due to the shape of the slot and asymmetric placement of the DRs, as discussed in the next section.

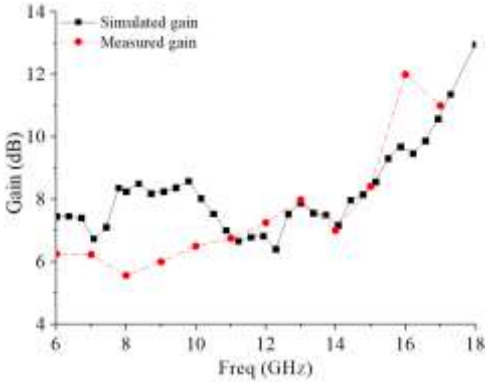

Fig. 7: Simulated and measured antenna gain of the antenna.

Figure 7 illustrates the simulated and measured antenna gains in the broadside direction of the antenna. The simulation assumes an ideal feeding network, whereas the measured result includes the insertion loss of the feeding network used, hence there are local discrepancies. The figure shows that the calculated gain varies between 6.46 dBi and 12.95 dBi with a maximum of 12.95 dBi at 17.64 GHz, while the measured gain varies between 5.56 dBi and 12 dBi across the band of 6 to 17 GHz. It can be seen that on average the measurements are comparable with the predictions, although a higher discrepancy is noticed across the range 7.5 to 10.5 GHz.

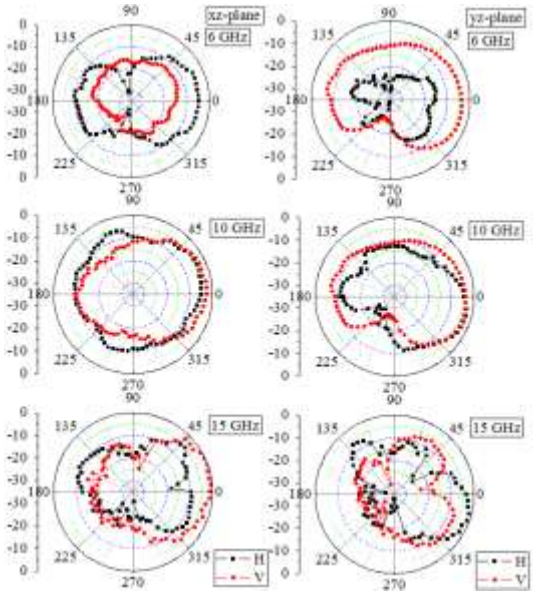

Fig. 8: Normalized measured radiation patterns; (a) in the XZ-plane, (b) in the YZ-plane.

Fig. 8 displays the normalized measured radiation patterns at frequencies of 6, 10 and 15 GHz. This indicates that the antenna has a wide radiation pattern with maximum radiation along the normal to the substrate covering half-space. It should be noted that the back radiation level is small as can be seen from the front to back ratio which in more than 10 dB. The radiation from the slot (back radiation of the antenna) is unavoidable, and depends on the electrical length of the slot at the frequency of operation. In this design, the length of each of the adjacent slots is 6.6 mm, which is equivalent to 0.33 of the free space wavelength at the highest frequency of operation of 15 GHz.

III. Interpretation of the Extended Bandwidth

The arrangement of two slots feeding the two DRs gives an extra degree of freedom in the design procedure. The higher bandwidth achieved can be interpreted as the result of merging many resonating frequencies bands due to the parts constituting the antenna. Obviously, adding a second slot has resulted in an increased bandwidth. When these frequencies are related to the relevant parts of the antenna, then the designer has wider scope to tailor the required extension of the bandwidth. The resonating parts of the antenna are DRs, slots, and feed line/stub. Here are notes about these parts:

A- The effect of a single DR

The empirical formula used (see equation 1 above) cannot predict the higher modes of the DR.

The other formula which gives the resonance frequencies of the TM_{11m} modes is [34]:

$$f_{npm} = \frac{c}{2a\pi\sqrt{\varepsilon_r}}\sqrt{X_{11}^{'2} + \left(\frac{\pi a}{2h}(2m+1)\right)^2} \quad (2)$$

where $D = 2a$ is the diameter of the CDR, h is the height of the CDR, ε_r is the relative permittivity of the CDR material, c is the velocity of light, and, for the TM_{11m} modes, $X'_{11} = 1.84$. For the particular DR used, the resonance frequencies are 9.936 GHz for the TM_{110} mode, 12.56 GHz for the TM_{111} mode, and TM_{112} at 16.61 GHz, and the TM_{102} mode frequency 16.08 GHz. These modes are evident in the obtained simulation and experimental results. Thus, the source of the two dips in Fig. 5 is explained.

*B- **The effect of the two DR**s*

In this part, we replace the two cylindrical DRs by an equivalent rectangular one, as illustrated in Fig. 9. The dimensions of the equivalent rectangular DR are D×2D×h = 6×12×9 mm^3. It can be shown that, for the two DRs used the calculated equivalent relative permittivity is $\varepsilon_r^{rectangle} = 7.59$ Figure 10 compares the simulated S_{11} responses of the antenna with the two DRs and that with the equivalent rectangular DR. Good agreement is obtained up to a frequency of about 13.5 GHz

Fig. 9: the equivalent rectangular DR compared to the two DR cylindrical case.

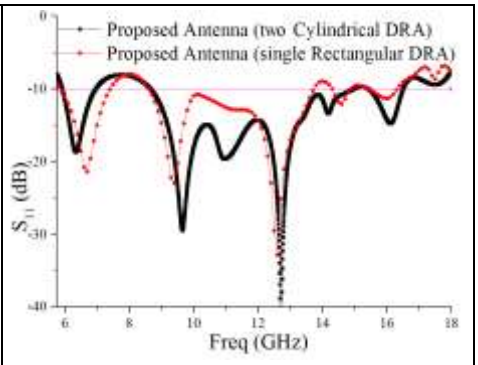

Fig. 10: Simulated reflection coefficients of the antenna with two cylindrical DRAs compared with the same antenna using a single equivalent rectangular DRA as presented in Fig. 9.

According to [34], the frequencies of the three fundamental modes $HEM_{01\delta}$, $TE_{01\delta}$ and $TM_{01\delta}$ are respectively: 10.484, 12.19 and 18.16 GHz, while according to [35, 36] the resonant frequencies for modes $HE_{11\delta}$, $EH_{11\delta}$, $TE_{01\delta}$ and $TM_{01\delta}$ are respectively 9.85, 10.24, 12.28 and 18.21 GHz. These modes are being excited by each of the two DRA alone. Therefore, it is possible for other modes that have low frequencies to be excited by the two DR combination (the same effect as the rectangular DRA).

With the rectangular DRA, according to [37, 38] the frequencies of $TE_{\delta 11}$, $TE_{1\delta 1}$, and $TE_{11\delta}$ (for a single resonator) are respectively 7.19, 10.22 and 10.51 GHz. One may conclude that both DRAs can generate and excite other modes below 10.5 GHz (as with a single DRA) for lower frequencies similar to the rectangular DRA combined with the larger slot. Fig. 10 shows that the benefit of using two DRs is the ability to have hybrid modes at lower frequencies, and that there are more of these than with a rectangular DRA (7.19, 9.84 and 10 GHz).

*C- **The effect of the slot***

A rectangular slot of length L_s that is short-circuited at both ends can have a first mode resonance when the slot length is equal to half the guided wavelength λ_g, i.e.

$$L_s = 0.5\lambda_g \quad (3)$$

The guided wavelength is given by:

$$\lambda_g = \frac{\lambda_0}{\sqrt{\varepsilon_{re}}} = \frac{c}{f\sqrt{\varepsilon_{re}}} \quad (4)$$

where f_r is the resonance frequency, and ε_{re} is the effective dielectric constant for the wave inside the slot, given by:

$$\varepsilon_{re} = \frac{\varepsilon_{rs}+1}{2} \quad (5)$$

Here ε_{rs} is the dielectric constant of the substrate material.

Combining equations 4, 5 and 6 gives:

$$f_r = \frac{c}{L_s\sqrt{2(\varepsilon_{rs}+1)}} \quad (6)$$

For the slot length used, L_s = 6.6 mm, f_r is 13.7 GHz. This frequency value is close (within 7%) to the resonance frequency of 12.7 GHz seen in the presented results. The shift in estimated frequency can be attributed to the following: Equation 6 assumes an average dielectric constant that is the mean of the air and substrate values, but when the DR is placed adjacent to the slot then the average value ε_{rs} will be higher, leading to a lower value of the frequency as compared to that given by Equation 7.

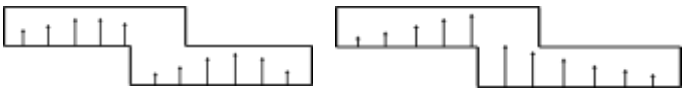

Fig. 11: The two adjacent rectangular slots can induce two cases of resonance.

The above reasoning assumes a rectangular slot. The use of two adjacent rectangular slots can result in two cases of resonance, see Fig. 11, where the electric fields of the resonating modes are indicated by arrows. The first case assumes two independent slots each of length L_s (see Fig. 11a) with each one resonating at the frequency given by equation 7. The second case is represented by an equivalent slot comprising the two merged slots, see Fig. 11b. This longer slot has an equivalent length value that is between L_s and 2 L_s depending on the overlap of the two slots. In our prototype, the slot length is about 6.6 mm, and the combined slot length 9.6 mm. This equivalent length leads to a resonance frequency of 9.4 GHz. Of course, this value will be affected by the proximity of the DR leading to a slightly lower value of frequency.

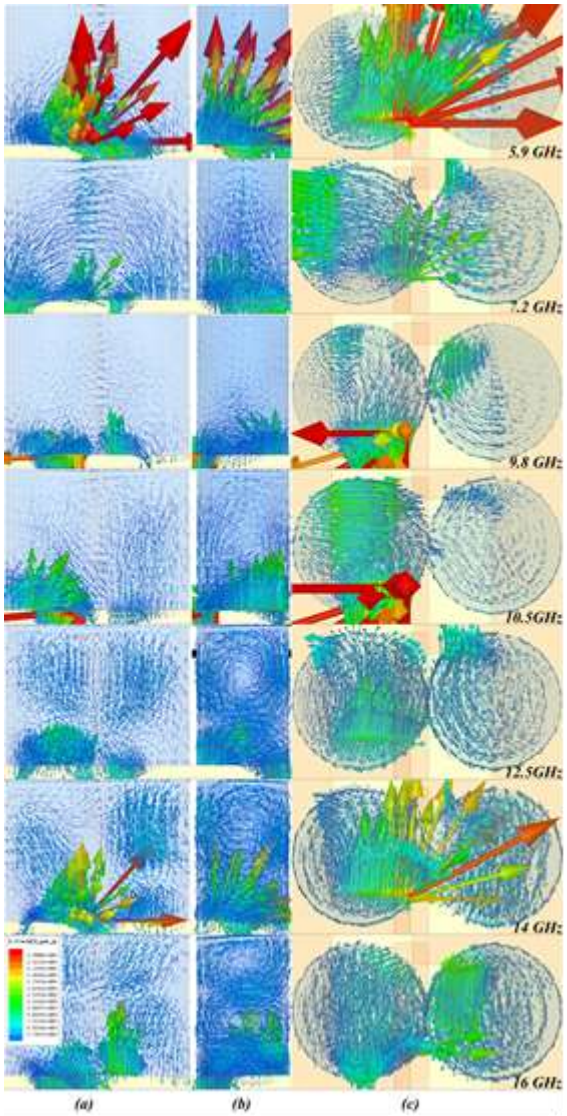

Fig. 12: Magnitude of the electric field distribution across ((a) xz plane, (b) yz plane and(c) xy plane) at 5.9 GHz, 7.2 GHz, 9.4 GHz, ($HEM_{01\delta}$ mode) 10.5 GHz, 14 GHz and 16.0 GHz ($TE_{\delta 21}$).

The lower band of frequencies results from the combined effects of the slot, single DR or the two DRs. The other element that may be considered in resonance calculations is the microstrip feed line. This line is connected between the 50Ω impedance input connector and a combination of open-end, slots and two DRs. In the lower frequency band, the feedline can be considered to work as 1/4 wavelength transformer. Thus a dip in the input reflection coefficient is noticed when the line length is equal to 1/4 or 3/4 of the guided wavelength. The substrate thickness is h = 0.8 mm. With a line width W = 1.5 mm, the effective dielectric constant using [39] it was found to be 3.39. For a feed line length of 21 mm, the resonance frequencies are 1.94 GHz for the 1/4 wave length case, and 5.82 GHz for the 3/4 wave length case. The second value of frequency is very near to the lower band (see Fig. 10), thus verifying the existence of the lower band.

*D- **The combined effect of the slot with DRAs in radiating modes***

From the input impedance (Fig. 6), it was feasible to plot the magnitude of electric field (on the three planes) at seven frequencies which have an important effect on the parameters of our structure. As shown in Fig. 12, at all the frequencies there is a very large coupling generated by the wide slot and the DRAs, especially at 5.9 GHz, the resonance frequency of the slot (3/4 wave length case).

A mode (quasi $TE_{\delta 11}$) at 7.2 GHz is generated by the slots and the two DRAs, which begins in one and finishes in the other DRA [37, 38].

Also in the 9.8 to 12.5 GHz range and around the resonance frequency of the slot at 12.7 GHz, each DRA reacts separately and resonates differently resulting in the first order mode, and the splitting of the modes $HEM_{01\delta}$, $TE_{01\delta}$, $HE_{11\delta}$, $EH_{11\delta}$, and $TE_{01\delta}$. The DRA therefore resonates at 10.5 GHz in the $HEM_{11\delta}$ mode. The $TE_{1\delta 1}$ mode generated by the two DRAs is also visible.

From the resonance frequencies of the higher order modes given in [34] and the shape of the E-field at frequencies 14 and 16 GHz, we find that these modes are: TE_{102} = 14.91 GHz, TM_{102} = 16.08 GHz and TM_{112} = 16.61 GHz. In general, we find that the two DRAs combine and manifest with the slot throughout the frequency band studied.

IV. Conclusions

A compact dielectric resonator antenna for ultra-wideband applications has been designed, fabricated and tested. The use of two DRs excited by two adjacent and displaced slots enhances the performance of the antenna, and the asymmetric location of the DR pair, together with the dimensions and the shape of the aperture, gives designers more freedom for optimization. Displacing the two DRs vertically and horizontally reveals optimum configurations, yielding antennas with better performances. In this study, an impedance bandwidth of about 53%, covering the frequency range from 8.72 to 15 GHz and a lower band from 5.9 to 7.32 GHz with relative bandwidth of 21.5%, and a maximum realized gain of 12 dBi were obtained.

References

[1] V. Rabinovichand and N. Alexandrov,"Antenna Arrays and Automotive Applications", Springer, 2013.

[2] M. G. N. Alsath and M. Kanagasabai, “Compact UWB Monopole Antenna for Automotive Communications”, IEEE Trans on Antennas and Propagation, vol. 63, No. 9, pp. 4204-4208, Sept 2015.

[3] M. Martinez, A. Winkelmann and R. Baggen, (2010), *Antennas for Automotive Applications* [Online]. Available: http://www.antennasvce.org /Community/Dissemination/get_file?id_file = 312

[4] D. Guha; M. Biswas; Y. M. M. Antar, "Microstrip patch antenna with defected ground structure for cross polarization suppression", IEEE Antennas and Wireless Propagation Letters, Vol. 4, Issue: 1, pp. 455 – 458, 2005.

[5] C. Kumar and D. Guha, "Defected ground structure (DGS)-integrated rectangular microstrip patch for improved polarization purity with wide impedance bandwidth", IET Microwaves, Antennas & Propagation, 8 (8), pp. 589-596, 2014.

[6] D. Guha, S. Biswas, and et al, "Defected ground structure to reduce mutual coupling between cylindrical dielectric resonator antennas", Electronic Lett., Vol. 44, No.14, pp. 836-837, 2008.

[7] D. Guha, A. Banerjee, C. Kumar, Y. M. M. Antar,"New technique to excite higher order radiating mode in a cylindrical dielectric resonator antenna", IEEE Antennas and Wireless Propagation Letters, Vol. 13, pp. 15-18, 2014.

[8] D. Guha; P. Gupta; C. Kumar,"Dualband Cylindrical Dielectric Resonator Antenna Employing HEM11δ and HEM12δModes Excited by New Composite Aperture", IEEE Transactions on Antennas and Propagation, Vol. 63, Issue: 1, pp. 433 – 438, 2015

[9] I.T.E. Elfergani, A. S. Hussaini, and et.al., Printed Monopole Antenna with Tunable Band-Notched Characteristic for Use in Mobile and Ultra-Wide Band Applications, International Journal of RF and Microwave Computer-Aided Engineering. Vol. 25, No. 5, pp. 403-412, June 2015.

[10] A.A. Kishk, Y. Yin and A.W. Glisson, "Conical Dielectric Resonator Antennas for Wideband Applications", IEEE Trans. Antennas Propagation, Vol. 50, pp. 469-474, 2002.

[11] A.H. Majeed, A.S. Abdallah, and et al, "Aperture-Coupled Asymmetric Dielectric Resonator Antenna for Wideband Applications", IEEE Ant. and Wireless Propag. Letters, Vol. 13, pp. 927-930, May 2014.

[12] S.A. Long, M. W. McAllister and L. C. Shen, "The Resonant Cylindrical Dielectric Cavity Antenna", IEEE Trans. Antennas Propag., Vol. AP-31, No. 3, pp. 406-412, 1983.

[13] Y. Gao, Z. Feng and Li Zhang, "Compact Asymmetrical T-shaped Dielectric Resonator Antenna For Broadband Applications", IEEE Trans. Antennas Propagation, Vol. 60, issue 3, pp. 1611-1615, 2012.

[14] A. A. Kishk, "Wideband Dielectric Resonator Antenna in A Truncated Tetrahedron form Excited by A Coaxial Probe", IEEE Trans. Antennas Propagation, Vol. 51, no. 10, pp. 2907-2912, Oct. 2003.

[15] S. S. Yang, R. Chair, and et.al., "Study on Sequential Feeding Networks for Sub-Arrays of Circularly Polarized Elliptical DRA", IEEE Trans. Ant. and Propag. Vol. 55, No. 2, pp. 321-333, 2007.

[16] D. Guha, B. Gupta and Y. M. M. Antar. "Hybrid Monopole-DRAs Using Hemispherical/Conical-shaped Dielectric Ring Resonators: Improved Ultra Wide Band Designs", IEEE Trans. Antennas Propagation, Vol. 60, Issue 1, pp. 393-398, 2012.

[17] K. S. Ryu and A. A. Kishk, "Ultrawideband Dielectric Resonator Antennas", International workshop on Antenna Technology, Lisbon, pp. 1-4, March 2010.

[18] C Zebiri, F. Benabelaziz, and et.al., "Aperture-Coupled Asymmetric Dielectric Resonator Antenna with Slotted Microstrip line for Enhanced Ultra-Wideband", The 10th European Conf. on Antennas and Propagation (EuCAP), Davos, Switzerland, pp. 1391-1394, 10-16 April 2016.

[19] M. R. Nikkhah, J. Rashed-Mohassel and A. A. Kishk, "High-Gain Aperture Coupled Rectangular Dielectric Resonator Antenna Array Using Parasitic Elements", IEEE Trans. Antennas Propagation, Vol. 61, No. 7, pp. 3905 – 3908, July 2013.

[20] M. J. Al-Hasan, T. A. Denidni and A. R. Sebak, "Millimeter-Wave EBG-Based Aperture-Coupled Dielectric Resonator Antenna", IEEE Trans. on Antennas and Propagation, Vol. 61, No. 8, pp. 4354 – 4357, August 2013.

[21] Q. Lai, C. Fumeaux, W. Hongand and R. Vahldieck, "60 GHz Aperture-Coupled Dielectric Resonator Antennas Fed by a Half-Mode Substrate Integrated Waveguide", IEEE Trans. Antennas Propagation, Vol. 58, No. 6, pp. 1856 – 1864, June 2010.

[22] R. N. Simons and R. Q. Lee, "Effect of Parasitic Dielectric Resonators on CPW/aperture Coupled Dielectric Resonator Antennas", IET Microw. Antennas Propag. vol. 140, no. 5, pp. 336–338, Oct. 1993.

[23] A. S. Al-Zoubi, A. A. Kishkand A. W. Glisson, "Aperture Coupled Rectangular Dielectric Resonator Antenna Array Fed by Dielectric Image Guide", IEEE Trans. on Ant. and Propag., Vol. 57, No. 8, pp. 2252-2259, Aug. 2009.

[24] K.W. Leung, Z.N. Chen, K.M. Luk and E.K.N. Yung, "Aperture-Coupled Dielectric Resonator Antenna with a Thick Ground Plane", IEEE Trans. on Ant. and Propag., Vol. 46, No. 8, pp. 1242-1243, Aug. 1998.

[25] Y. M. M. Antar and Z. Fan, "Theoretical Investigation Of Aperture-Coupled Rectangular Dielectric Resonator Antenna", Proc. Inst. Elect. Eng. Antennas Propag. Vol. 143, No. 2, pp. 113–118, Apr. 1996.

[26] K.W. Leung, K.M. Luk, K.Y.A. Lai and D. Lin, "Theory and Experiment of an Aperture Coupled Hemispherical Dielectric Resonator Antenna", IEEE Trans. on Antennas and Propagation., Vol. 43, No. 9, pp. 1192–1198, Nov. 1995.

[27] N. I. Dzulkipli, M. H. Jamaluddin, and M. F. M. Yusof, "Design of alphabet shaped slot-loaded dielectric resonator reflect array antenna at 12 GHz", IEEE Asia-Pacific Conference on Applied Electromagnetics (APACE), 2012, PP. 334-337.

[28] M. I. A. Sukur, M. K. A. Rahim, and N. A. Murad, "Bandwidth enhancement of rectangular dielectric resonator antenna using circular slot coupled technique", Microwave and Optical Technology Letters, 2016, Vol. 58, No 3, PP. 505-509.

[29] M. Leib, A. Vollmer, and W. Menzel, "An ultra-wideband dielectric rod antenna fed by a planar circular slot", IEEE Trans Microwave Theory Tech., Vol. 59, 2011, PP. 1082–1089.

[30] A.A. Kalteh, G.R.D. Salleh, M.N. Moghadisi, and B.S. Virdee, "Ultra wideband circular slot antenna with reconfigurable notch band function", IET Microwave Antennas Propag., Vol. 6 , 2012, PP. 108–112.

[31] P. Li, J. Liang, and X. Chen, "Study of printed elliptical/circular slot antennas for ultrawideband applications", IEEE Trans. Antennas Propag, Vol. 54, 2006, pp. 1670–1675.

[32] G. P. Junker,A. A. Kishk and A. W. Glisson, "Input Impedance of Aperture-Coupled Dielectric Resonator Antennas", IEEE Trans. Antennas Propagation, Vol.44, No. 5, pp. 600-607, May 1996.

[33] J.T.H. ST. Martin, Y. M. M. Antar, A. A. Kishk, A. Ittipiboon and M. Cuhaci, "Dielectric Resonator Antenna using Aperture Coupling", *Electron. Lett.* Vol. 26, pp. 2015–2016, Sep. 1990.

[34] K-M Luk and K-W Lueng, Eds., "Dielectric Resonator Antennas", Research Studies Press Ltd, Baldock, Hertfordshire, England, 2002.

[35] A.A. Kishk, A. Ittipiboon, Y.M.M. Antar and M. Cuhaci, "Slot excitation of the dielectric disk resonator", IEEE Trans. Antennas Propagation, Vol. 43, No. 2, pp. 198–201, 1995.

[36] R.K. Mongiaet and P. Barthia, "Dielectric Resonator Antennas - A Review And General Design Relations For Resonant Frequency And Bandwidth", International Journal Of Microwave And Millimeter-Wave Computer-Aided Engineering, Vol. 4, No. 3, pp. 230-247, 1994.

[37] A.A. Kishk, A.W. Glisson and G.P. Junker, "Study of Broadband Dielectric Resonator Antennas", Antenna applications symposium, Allerton Park, Monticello (Il), pp. 45-68, Sept 1999.

[38] R.K. Mongiaet and A. Ittipiboon, "Theoretical and Experimental Investigations on Rectangular Dielectric Resonator Antennas", IEEE Trans. Ant. And Propag., Vol. 45, No. 9, pp. 1348-1356, Sept., 1997.

[39] G. Kumar and K. P. Ray, "Broadband microstrip antennas", Artech House, Boston, London, 2003.